Evaluating Robust Constant Switching Frequency Direct Torque Control for Doubly Fed Induction Motor

DJAMILA CHERIFI, YAHIA MILOUD
Department of Electrical,
Engineering University of Dr.Tahar Moulay,
P. O. B. 138, 20000 Ennasr, Saida,
ALGERIA

Abstract: - This research presents an improved direct torque control (DTC) approach for a doubly-fed induction machine (DFIM) with two two-level voltage source inverters (VSI). One of the best control schemes to regulate the torque of the DFIM is the conventional direct torque control, or C-DTC. However, the low switching frequency of the DTC results in significant torque and flux ripples, which create acoustic noise that impairs the control performance, especially at low speeds. To address these limitations, the SVM-DTC technique is designed and simulated using MATLAB/Simulink to ensure full reference tracking, fast response, proper dynamic behavior, and low ripple level. The simulation results demonstrate how well the SVM-DTC control works for the DFIM in terms of speed, stability, and robustness.

Key-Words: - Doubly fed induction motor; direct torque control; ripple; two-level voltage inverter*;* space vector modulation.

Received: March 18, 2025. Revised: June 13, 2025. Accepted: July 11, 2025. Published: October 23, 2025.

1 Introduction

The doubly fed induction machine holds a significant position in industrial applications with variable speed because of its durability, structural simplicity, performance, weight, and affordability, [1], [2]. Its mathematical model is highly complex, multi-variable, and non-linear because of the coupling between the flux and the electromagnetic torque, despite the mechanical structure's simplicity, [3]. Due to these limitations, more sophisticated control algorithms are needed to regulate the machine's torque and flux in real time; many methods have been put forth to do this. Field-oriented control (FOC), another name for vector control, was proposed in [4], in the 1970s and claimed that it could adjust torque and flux independently, much like a separate excitation DC machine. A good transient response is achieved by working in both stable and dynamic settings thanks to the vector representation of the motor variables. All quantities will show up as DC quantities in the FOC control method that is based on the translation to the synchronous frame. However, the primary drawbacks of FOC are its sensitivity to changes in machine characteristics, such as the resistances of the stator and rotor, and its requirement for the flux angle, which cannot be measured directly, [5], [6]. One of the intriguing control schemes as a substitute for vector control in DFIM is the direct torque control approach (DTC). In the mid-1980s, the authors in Japan, [7], [8], and in Germany, [9], [10], under the name Direct Self-Control (DSC). This control is completely done in a stationary frame (stator fixed coordinates), in contrast to FOC. Furthermore, DTC generates the inverter gating signals directly through a look-up switching table, and the use of a modulator is not necessary. The advantages of this technique are the Fast dynamic response, the greatly reduced use of machine parameters, and a simple control. However, the standard DTC technique suffers from excessive flux and torque ripples owing to the usage of hysteresis controllers, [11], [12]. To counter these shortcomings, various enhancements have been developed to Direct Control approaches, such as the inclusion of the space vector modulation (SVM). Despite its complexity, the SVM-DTC approach lowers the high ripple level, [13], [14].

The two-phase mathematical model of the doubly fed induction machine is introduced in Section 2 of this study. The design of the traditional direct torque control of DFIM is explained in Section 3. A space vector modulation approach (SVM-DTC) for direct torque control of DFIM is introduced in sections 4 and 5. Section 6 presents and interprets the findings of the simulation, a Comparative study in Section 7. Lastly, the paper's conclusions are summed up in section 8.

2 DFIM Model

The two-phase model, expressed in (α, β) coordinates, serves as the ideal framework for analyzing dynamic characteristics, designing, and implementing direct torque control for the Doubly Fed Induction Motor (DFIM).

The corresponding equations outline this approach in detail:

$$\frac{d}{dt}\begin{bmatrix} i_{s\alpha} \\ i_{s\beta} \\ i_{r\alpha} \\ i_{r\beta} \end{bmatrix} = \left(\frac{1}{\sigma L_s L_r}\right) \cdot \begin{bmatrix} -r_s l_r & \omega_r M^2 & r_r M & \omega_r M l_r \\ -\omega_r M^2 & -R_s l_r & -\omega_r M l_r & r_r M \\ R_s M & -\omega_r l_s M & -R_r l_s & -\omega_r l_r l_s \\ \omega_r l_s M & r_s M & \omega_r l_r l_s & -r_r l_s \end{bmatrix} \cdot \begin{bmatrix} i_{s\alpha} \\ i_{s\beta} \\ i_{r\alpha} \\ i_{r\beta} \end{bmatrix} + \left(\frac{1}{\sigma l_s l_r}\right) \cdot \begin{bmatrix} l_r & 0 & -M & 0 \\ 0 & l_r & 0 & -M \\ -M & 0 & l_s & 0 \\ 0 & -M & 0 & l_s \end{bmatrix} \cdot \begin{bmatrix} v_{s\alpha} \\ v_{s\beta} \\ v_{r\alpha} \\ v_{r\beta} \end{bmatrix} \quad (1)$$

$i_{s\alpha}$, $i_{s\beta}$, $i_{r\alpha}$, $i_{r\beta}$ are stator and rotor currents components.
R_s , R_r are the stator and rotor resistance.
L_s , L_r are the stator and rotor inductance.
M is the mutual stator-rotor inductance
σ is the Blondel's coefficient.
ω_r is the machine speed
$v_{s\alpha}, v_{s\beta}, v_{r\alpha}, v_{r\beta}$ are stator and rotor voltages.

The electromagnetic torque expression of DFIM as a function of the stator flux and the stator currents is written as follows:

$$T_{em} = p\left(\phi_{s\alpha} i_{s\beta} - \phi_{s\beta} i_{s\alpha}\right) \quad (2)$$

where: $\phi_{s\alpha}$, $\phi_{s\beta}$ are stator flux components.

The fundamental equation of dynamics is:

$$T_{em} - T_L = J\frac{d\Omega}{dt} + f\,\Omega \quad (3)$$

A well-established technology that is quickly becoming an industry standard in response to the need for energy conservation is the two-level, three-phase voltage source inverter (VSI). Thanks to regulated transistor switches, the rectifier's output phase voltages (V_{dc}) are sent to the inverter's input, which transforms them into a three-phase AC voltage signal with a wide range of variable voltage amplitude and frequency.

The inverter's power and switching frequency determine the type of switches that are employed. IGBT transistors with anti-parallel diodes are very useful in the majority of applications.

Figure 1 shows the structure of a DFIM fed by two inverters at two levels.

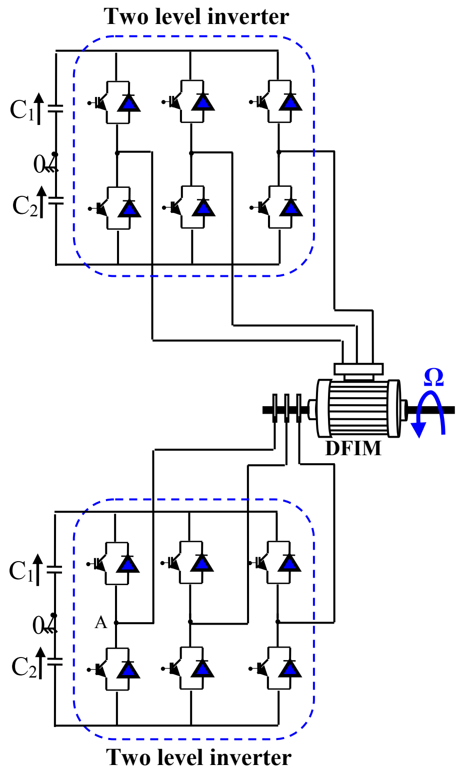

Fig. 1: Diagram of a DFIM and its power supply
Source: created by the authors

The doubly fed motor is supplied by two inverters, one at the stator and one at the rotor, as seen in Figure 1. Six transistor switches, S_1 through S_6, and a constant voltage source V_{dc} that connects a three-phase load make up each inverter, which is a three-phase, two-level voltage source (VSI).

The following formula creates the voltage vector:

$$\vec{V}_s = \sqrt{\frac{2}{3}} \mathrm{V}_{\mathrm{dc}} \left[S_a + S_b e^{j\frac{2\pi}{3}} + S_c e^{j\frac{4\pi}{3}} \right] \quad (4)$$

where the logical values of the three-phase inverter switching functions, S_a, S_b, and S_c, are 0 or 1.

3 Direct torque Control

The decoupling control of the flux and electromagnetic torque in the stationary frame (α, β) is accomplished by the direct torque control principle. It makes DFIM less susceptible to machine parametric fluctuations and enables a precise and quick electromagnetic torque response. Directly applying a control sequence to the voltage inverter's switches is the foundation of DTC control.

To choose the right voltage vector, it makes use of a switching table. The choice of switching states has a direct bearing on how the machine's torque and flux vary. Therefore, the torque and flux magnitudes are limited to two hysteresis bands in order to make the selection. Both of these amounts are separately regulated by those controllers, [15], [16].

Several parameters need to be established in order to guarantee satisfactory performance. The stator and rotor currents are measured, and the stator and rotor voltages are dependent on the DC link voltage and the switching state (S_a, S_b, and S_c) generated by the switching table. The coordinates (α,β) that are converted from these parameters are appropriately adjusted for the DTC control. The decoupling control of the flux and electromagnetic torque in the stationary frame (α, β) is accomplished by the direct torque control principle. It makes DFIM less susceptible to machine parametric fluctuations and enables a precise and quick electromagnetic torque response. Directly applying a control sequence to the voltage inverter's switches is the foundation of DTC control. To choose the right voltage vector, it makes use of a switching table. The choice of switching states has a direct bearing on how the machine's torque and flux vary. Therefore, the torque and flux magnitudes are limited to two hysteresis bands in order to make the selection. Both of these amounts are separately regulated by those controllers, [17].

Several parameters need to be established in order to guarantee satisfactory performance. The stator and rotor currents are measured, and the stator and rotor voltages are dependent on the DC link voltage and the switching state (S_a, S_b, and S_c) generated by the switching table. The coordinates (α,β) that are converted from these parameters are appropriately adjusted for the DTC control.

In order to implement the DTC concept, the torque supplied by the DFIM must be changed in order to continuously regulate the stator and rotor flux. The DFIM flow expressions are represented by the above equations, [18], [19], [20]:

$$\begin{cases} \vec{\varphi}_s = \int_0^t (\vec{v}_s - r_s\vec{I}_s)dt + \vec{\varphi}_{s0} \\ \vec{\varphi}_r = \int_0^t (\vec{v}_r - r_r\vec{I}_r)dt + \vec{\varphi}_{r0} \end{cases} \tag{5}$$

with: φ_s , φ_r are the stator and rotor flux components.

In the relations of the voltages V_s and V_r, we can ignore the expressions $r_s. I_s$ and $r_r. I_r$. As a result, the stator and rotor fluxes can be expressed as follows:

$$\begin{cases} \vec{\varphi}_s = \int_0^t \vec{v}_s dt + \vec{\varphi}_{s0} \\ \vec{\varphi}_r = \int_0^t \vec{v}_r dt + \vec{\varphi}_{r0} \end{cases} \tag{6}$$

3.1 The electromagnetic Torque Control Principle

The following is an expression for the relationship between the electromagnetic torque and the vector product of the stator and rotor flux vectors, [21], [22]:

$$T_{em} = K(\vec{\varphi}_s \times \vec{\varphi}_r) = K|\vec{\varphi}_s|.|\vec{\varphi}_r|.\sin(\gamma) \tag{7}$$

with:

K: is a constant that is contingent upon the machine's settings.

$$K = \frac{3pM}{2(\sigma.l_s.l_r)}$$

3.2 Estimators

3.2.1 Estimation of Stator and Rotor Flux

By examining the machine's voltage and current readings, the flux can be approximated. Considering the equations, [23]:

$$\vec{\varphi}_s(t) = \int_0^t \left(\vec{v}_s - r_s\vec{I}_S\right)dt \tag{8}$$

The two-axis, two-phase components (α, β) of the stator must be calculated to get the flux vector, so that:

$$\vec{\varphi}_s = \vec{\varphi}_{s\alpha} + j\vec{\varphi}_{s\beta} \tag{9}$$

With:

$$\begin{cases} \hat{\varphi}_{s\alpha} = \int_0^t (v_{s\alpha} - r_s I_{s\alpha})dt \\ \hat{\varphi}_{s\beta} = \int_0^t (v_{s\beta} - r_s I_{s\beta})dt \\ \hat{\varphi}_{r\alpha} = \int_0^t (v_{r\alpha} - r_r I_{r\alpha})dt \\ \hat{\varphi}_{r\beta} = \int_0^t (v_{r\beta} - r_r I_{r\beta})dt \end{cases} \tag{10}$$

The stator and rotor flux magnitudes are expressed as follows, [23]:

$$\hat{\varphi}_s = \sqrt{\hat{\varphi}_{s\alpha}^2 + \hat{\varphi}_{s\beta}^2} \tag{11}$$

$$\hat{\varphi}_r = \sqrt{\hat{\varphi}_{r\alpha}^2 + \hat{\varphi}_{r\beta}^2} \tag{12}$$

An equivalent value is represented by the angle α_s produced between the stator frame and the vector $\bar{\phi}_s$.

$$\alpha_s = arctg\left(\frac{\hat{\varphi}_{s\alpha}}{\hat{\varphi}_{s\beta}}\right) \tag{13}$$

The position of the rotor flux is calculated from:

$$\alpha_r = arctg\left(\frac{\hat{\phi}_{r\beta}}{\hat{\phi}_{r\alpha}}\right) \tag{14}$$

The Concordia transformation is applied to the measured currents in order to break down the stator current vectors $I_{s\alpha}, I_{s\beta}$ into their constituent parts.

$$\bar{I}_s = I_{s\alpha} + jI_{s\beta} \tag{15}$$

with: $$\begin{cases} I_{s\alpha} = \sqrt{\dfrac{3}{2}} I_{sa} \\ I_{s\beta} = \sqrt{\dfrac{1}{2}} (I_{sb} - I_{sc}) \end{cases}$$

Applying the Concordia transformation to the observed input voltages V_{an}, V_{bn}, and V_{cn} yields the components $v_{s\alpha}$ and $v_{s\beta}$. The command states (S_a, S_b, and S_c) dictate the voltages, which are obtained from the inverter's input voltage V_{dc}:

$$\vec{v}_s = v_{s\alpha} + jv_{s\beta} \tag{16}$$

with: $$\begin{cases} v_{s\alpha} = \sqrt{\dfrac{2}{3}} V_{dc} \cdot \left[S_a - \dfrac{1}{2}(S_b + S_c) \right] \\ v_{s\beta} = \dfrac{1}{\sqrt{2}} V_{dc} \cdot (S_b - S_c) \end{cases}$$

3.2.2 Electromagnetic Torque Estimation

The following form can be used to express the electromagnetic torque, [23]:

$$\hat{T}_{em} = p.(\hat{\varphi}_{s\alpha}.I_{s\beta} - \hat{\varphi}_{s\beta}.I_{s\alpha}) \tag{17}$$

According to the relationship displayed, the predicted torque amplitude depends on the current measurement as well as the stator flux estimator.

The resulting look-up table for DTC, which was proposed by Takahashi, is presented in Table 1.

Table 1. Look-up table for basic direct torque control

flux	Torque	1	2	3	4	5	6	comparator
Cflx =1	Ctrq=1	V_2	V_3	V_4	V_5	V_6	V_1	Tow-level
	Ctrq=0	V_7	V_0	V_7	V_0	V_7	V_0	
	Ctrq=-1	V_6	V_1	V_2	V_3	V_4	V_5	Three level
Cflx =0	Ctrq=1	V_3	V_4	V_5	V_6	V_1	V_2	Tow-level
	Ctrq=0	V_0	V_7	V_0	V_7	V_0	V_7	
	Ctrq=-1	V_5	V_6	V_1	V_2	V_3	V_4	Three level

Source: [7]

3.3 Global Scheme of Basic Direct Torque Control

Figure 2 displays the fundamental direct torque control strategy's global control scheme. It is made up of a proportional-integral (PI) controller for speed regulation and a speed regulation loop. The process is carried out by contrasting the measured speed value with the speed reference signal. The PI controller then uses the comparison error as its input. The controller gains are calculated using the pole positioning method. A two-level hysteresis comparator is used to produce the binary variable $(H_\phi = 0{,}1)$ at its output, which represents the intended evolution for the flux, when the error (e_ϕ) between the reference flux and estimated flux is introduced.

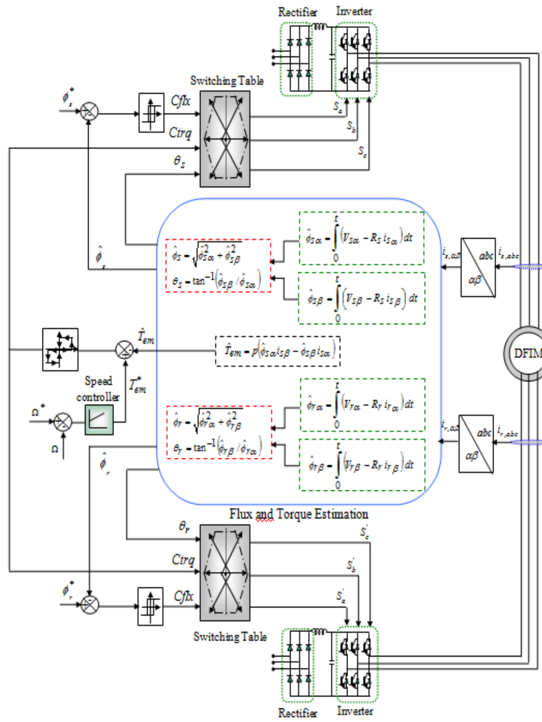

Fig. 2: Synoptic schema of conventional direct torque control of DFIM
Source: created by the authors

Similar to this, the torque's immediate error $(e_{T_{em}})$ is determined by comparing its estimated value $(\hat{T}_{em})$ with its reference value (T^*_{em}). This value is then applied to a three-level hysteresis comparator, which produces the variable $(H_{T_{em}})$ at its output with three levels (-1,0,1), which indicates the desired direction of the torque's temporal evolution.

3.4 Simulation Results and Interpretations

To demonstrate the effectiveness of the proposed control algorithm, incorporated into a DTC-controlled DFIM speed control system, speed regulation with load disturbances was simulated.

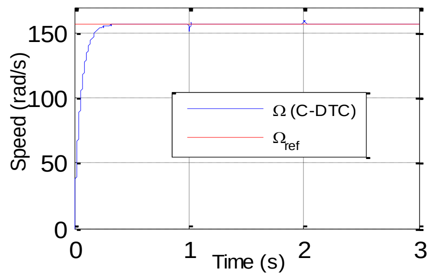

Fig. 3: Speed response for conventional DTC
Source: created by the authors

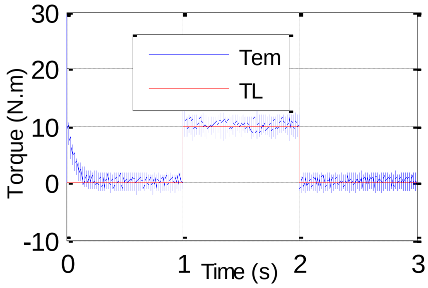

Fig. 4: Torque response for conventional DTC
Source: created by the authors

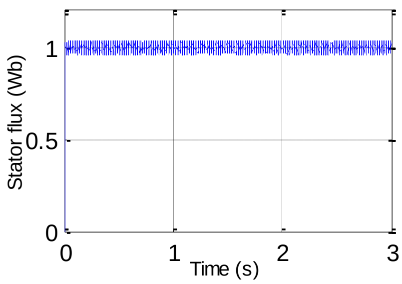

Fig. 5: Stator Flux response for conventional DTC
Source: created by the authors

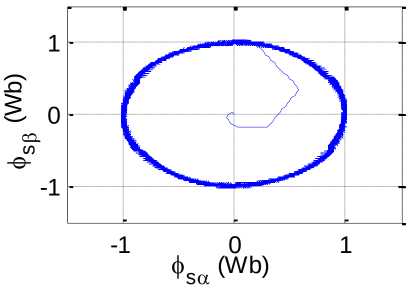

Fig. 6: Evolution of the stator flux in the reference frame (α, β) for conventional DTC
Source: created by the authors

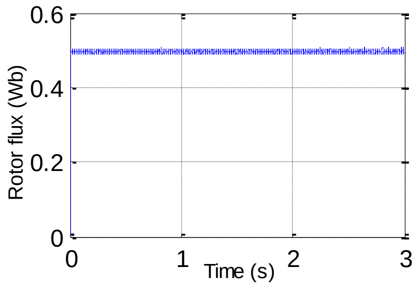

Fig. 7: Rotor Flux response for conventional DTC
Source: created by the authors

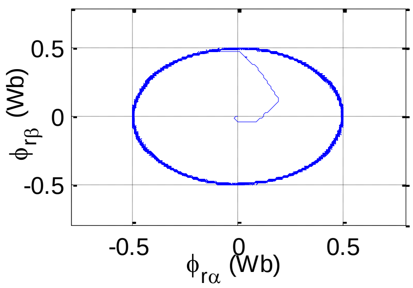

Fig. 8: Evolution of the rotor flux in the reference frame (α, β) for conventional DTC
Source: created by the authors

The general ideas of the classical DTC of a doubly fed asynchronous machine have been introduced in this section. An intriguing answer to the robustness issues is offered by this method. This form of control's primary benefit is that it eliminates the requirement for a sensor by enabling control over the machine's torque and flux as shown by the simulation results in Figure 3, Figure 4, Figure 5, Figure 6, Figure 7 and Figure 8. However, because the switching frequency varies, this control exhibits significant oscillations in these two parameters (torque and flux). The SVM DTC will be used in the next section of this work to enhance the DFIM's traditional DTC control's performance in terms of reducing ripples.

4 Constant Switching Frequency Direct Torque Control using SVM

Variable switching frequency and strong torque and flux ripples are common characteristics of typical DTC performance. This study has focused on modifying the traditional DTC approach by adding a vector modulator in order to get around these problems. A voltage vector with a fixed switching frequency is applied using the vector PWM approach (SVM), [24], [25]. To regulate the stator flux and electromagnetic torque, the control system uses proportional and integrating controllers (PI) in place of the switching table and hysteresis comparators.

4.1 Space Vector Modulation Algorithm

In the latter part of the 1980s, a group of German researchers introduced the SVM technique. The theory and application of SVM approaches have been the subject of extensive research since then. Better DC bus usage, less torque ripple, reduced Total Harmonic Distortion (THD) in the AC motor current, reduced switching losses, and ease of implementation in digital systems are only a few benefits of SVM approaches. By projecting the reference vector between adjacent vectors that correspond to two non-zero switching states, SVM predicts the inverter voltage vector, [26], [27]. As seen in Figure 9, the switching vectors diagram for a two-level inverter creates a hexagon with six sectors, each of which is enlarged by 60°.

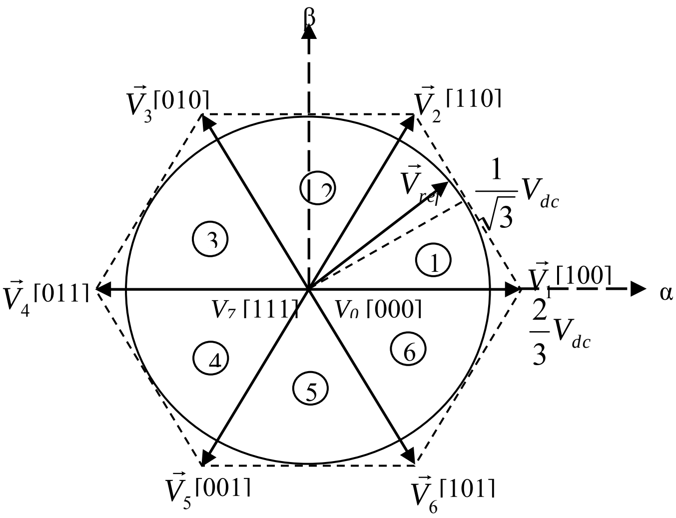

Fig. 9: Diagram of voltage space vector
Source: [28]

Vector computations can be used to determine the application time for each vector, and the null vector will be applied for the remaining time.

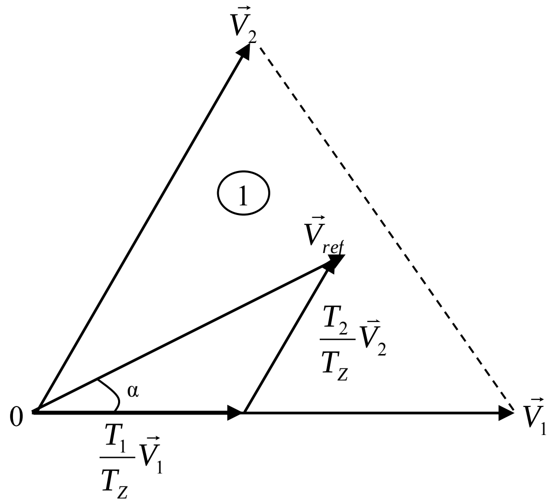

Fig. 10: Reference vector as a combination of adjacent vectors at sector 1
Source: [28]

The vectors V_1, V_2, and V_0 (zero vector) can be used to synthesize the reference voltage when it is in sector 1 (Figure 10).

Simple projections are used to determine timings T_1 and T_2, which correspond to voltage vectors:

$$T_1 = \frac{\sqrt{6}\cdot V_{s\alpha} - \sqrt{2}\cdot V_{s\beta}}{2V_{dc}} T \tag{18}$$

$$T_2 = \frac{\sqrt{2}\cdot V_{s\beta}}{V_{dc}}\cdot T \tag{19}$$

V_{dc}: DC bus voltage.

The voltage vectors' corresponding application timings are T_1, T_2, and T_0, respectively T_z is shown in Figure 11. The sample time is.

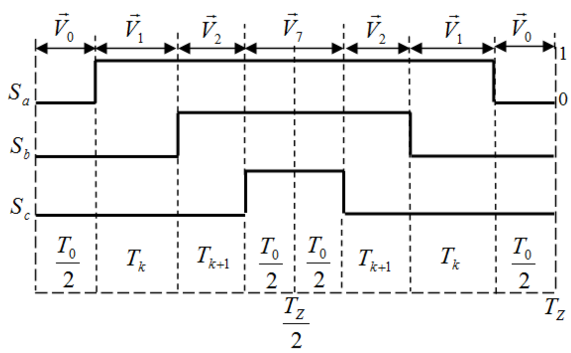

Fig. 11: Switching times of sector 1
Source: [28]

4.2 The Speed Control of the IM

Figure 12 displays the SVM direct torque control strategy's global control system. It is made up of a proportional-integral (PI) controller for speed regulation and a speed regulation loop. The process is carried out by contrasting the measured speed value with the speed reference signal. The PI controller then uses the comparison error as its input. The controller gains are calculated using the pole positioning method. The anti-windup controller is the PI controller that we employ in the outer speed loop. By eliminating the windup phenomenon brought on by the pure integrator's saturation, it enables improved speed control performance. The speed anti-windup PI controller schematic block is displayed in Figure 12.

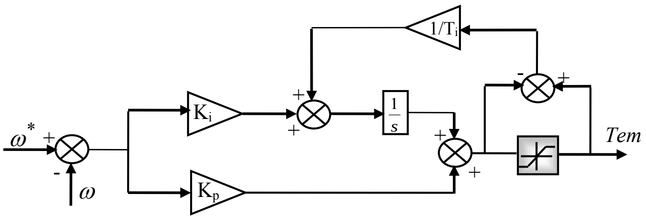

Fig. 12: Speed anti-windup PI controller
Source: created by the authors

This tactic involves adjusting the integral action according to the variation between the saturation limit and the control signal. Before reaching the integrator as feedback, the differential value is routed via a gain block (monitoring time constant T_i).

5 General Structure of Direct Torque Control by Vector Modulation (DTC_SVM)

Figure 13 shows the block diagram of the direct torque control of a doubly supplied asynchronous machine. This configuration consists of a three-phase DFIM powered by two two-level voltage inverters, one for the stator windings and the other for the rotor windings, with the use of the two SVM blocks, and a rotor speed control loop with an anti-windup PI corrector.

The DTC_SVM consists of replacing all hysteresis comparators with PI regulators and the commutation table with the SVM block. The inverter commutation states are generated by the SVM block from the reference stator and rotor voltages coming from the regulators.

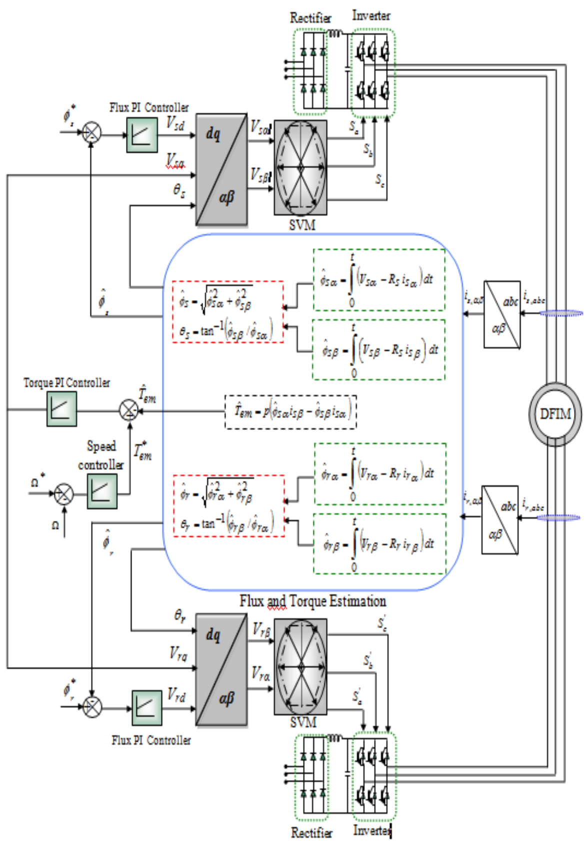

Fig. 13: Global control scheme of SVM- direct torque control of DFIM
Source: created by the authors

6 Simulation Results and Discussion

The numerical simulation results showing the behavior of the direct torque control by vector modulation (DTC_SVM) structure of the DFIM for the two cases—the first running at constant speed and the second at variable speed—are presented in this part to validate the suggested algorithm.

6.1 Test Number 1

The behavior of the drive system was simulated for a no-load start, followed by the introduction and removal of the load torque of 10N.m for a speed reference of $\Omega_{ref} = 150$ rad/s in order to illustrate the effectiveness of the DTC-SVM technique based on PI controllers.

The figures below show the results of the system studied:

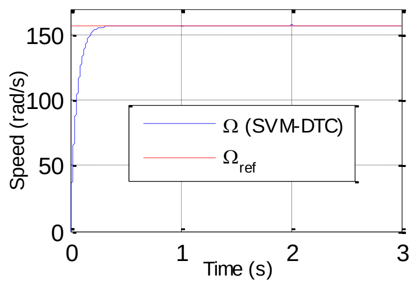

Fig. 14: Speed response
Source: created by the authors

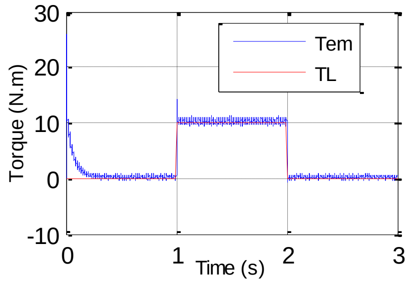

Fig. 15: Torque response
Source: created by the authors

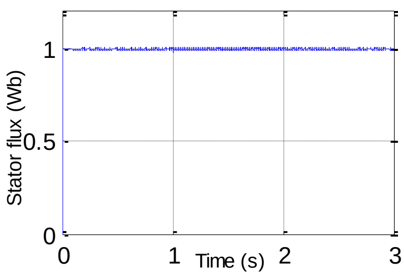

Fig. 16: Stator Flux Response
Source: created by the authors

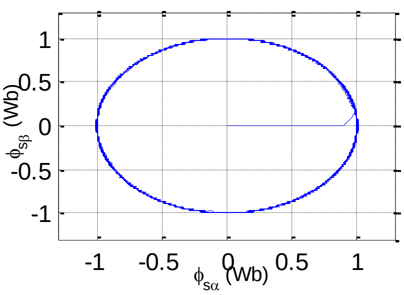

Fig. 17: Evolution of the stator flux in the reference frame (α, β)
Source: created by the authors

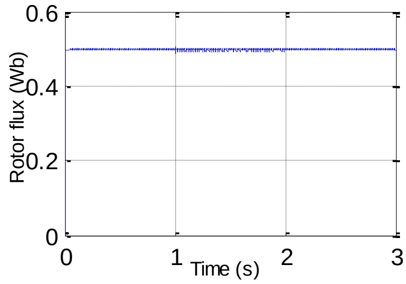

Fig. 18: Rotor Flux Response
Source: created by the authors

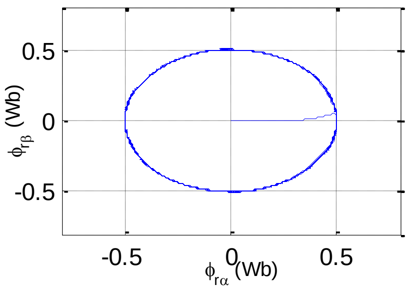

Fig. 19: Evolution of the rotor flux in the reference frame (α, β)
Source: created by the authors

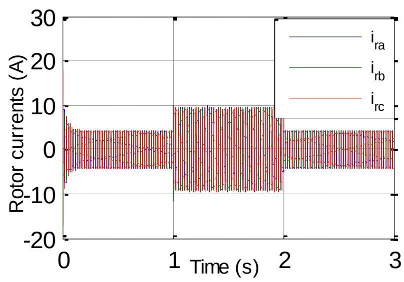

Fig. 20: Rotor Current Response
Source: created by the authors

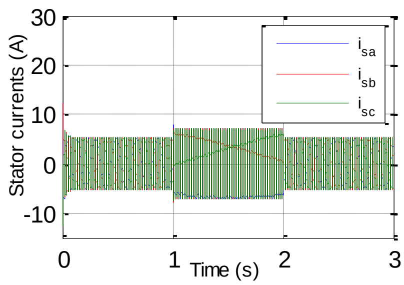

Fig. 21: Stator Current Response
Source: created by the authors

We observe that there is neither overshoot nor static error when the speed reaches its reference (Figure 14). Specifically, Figure 15 shows a significant reduction in torque ripples. In Figure 16, the amplitude of stator flux is constant. Figure 17 and Figure 19 show that the flux trajectory (stator and rotor) is nearly circular, meaning that its amplitude is constant in Figure 18.

The currents immediately establish themselves in the transition phase and respond well to the fluctuations imposed by the electromagnetic torque by retaining their sinusoidal shape. When comparing the DFIM powered by a voltage inverter controlled by the SVM approach to the standard DTC, we find a notable decrease in harmonics (Figure 20 and Figure 21).

These simulation results show how well the developed DTC-SVM technique performs.

6.2 Test Number 2

With the addition of the load torque of Cr=10N.m between the instants t1=1s and t2=2s, respectively, these simulation results for a test of reference change of speed of 150 rad/s at t=0.5s and of -150 rad/s at t=2.5s

The figures below show the results of the variable speed test:

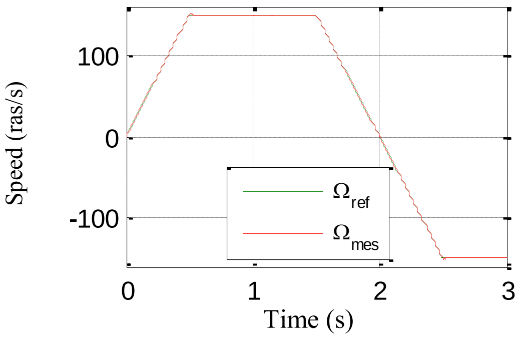

Fig. 22: Variable speed response
Source: created by the authors

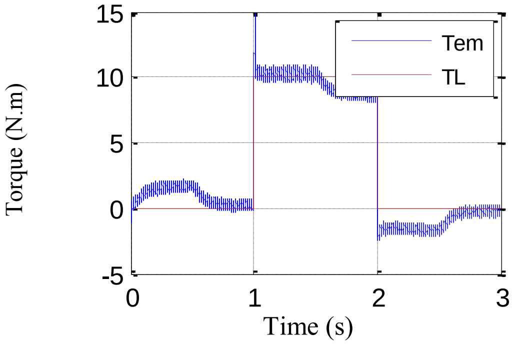

Fig. 23: Torque response for variable speed
Source: created by the authors

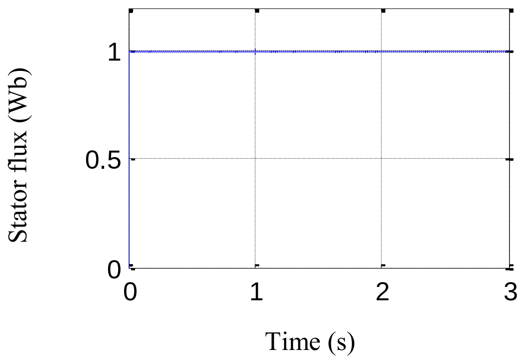

Fig. 24: Stator Flux response for variable speed
Source: created by the authors

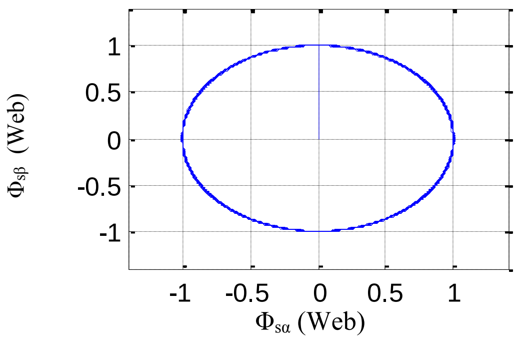

Fig. 25: Evolution of the stator flux in the reference frame (α, β) for variable speed
Source: created by the authors

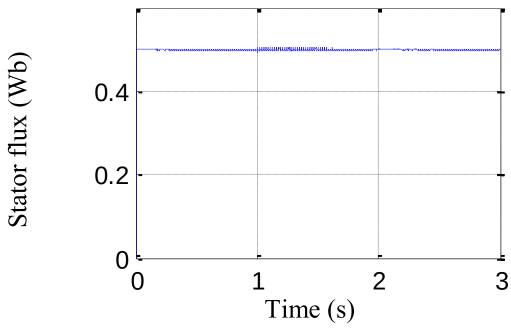

Fig. 26: Rotor Flux response for variable speed
Source: created by the authors

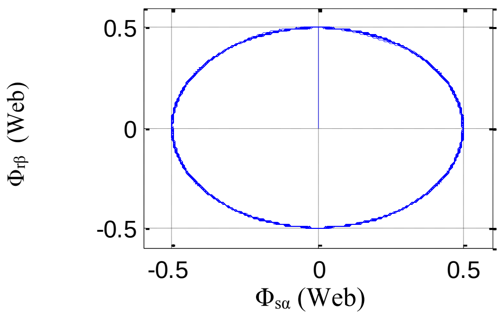

Fig. 27: Evolution of the rotor flux in the reference frame (α, β) for variable speed
Source: created by the authors

The simulation results in Figure 22, Figure 23, Figure 24, Figure 25, Figure 26 and Figure 27 show that the DFIM behaves well even when the load torque and rotational direction change. These findings further demonstrate the good decoupling between the torque and the fluxes, since the flux trajectory (stator and rotor) has a perfectly circular form and the stator and rotor fluxes remain constant at their references despite variations in the load torque. These findings unequivocally demonstrate the significant decrease in torque and flux ripples.

7 Comparative Study

A comparison of the two direct torque control methods for a DFIM suggested in this work to enhance these capabilities is summarized in Table 2.

Table 2. Two methods for enhancing direct torque control are compared

Performance index	Conventional DTC	DTC-SVM
Torque dynamic response	Fast	Fast
Torque ripple	High	Medium
Flux ripple	High	Medium
Current THD	More distortions	Less distortion
Regulation	hysteresis	PI conventional
Switching frequency	Variable	Constant
PWM Modulation	Not necessary	Necessary
Algorithm complexity	Simple	Simple

Source: [18]

8 Conclusion

Regarding changes in DFIM settings, direct torque control shows excellent resilience and dynamic performance. The direct determination of the control pulses given to the voltage inverter switches forms the basis of its operation. Nevertheless, there are two significant problems: first, the switching frequency is quite variable; second, the torque ripples' amplitude and the stator and rotor flux are not well controlled across the entire speed range of the intended operation. It should be mentioned that torque ripples disrupt the rotating shaft by producing extra noise and vibration.

The goal of this research project is to investigate a method for enhancing direct torque control performance. The robust DTC control algorithm, which is based on SVM control, is the focus of this paper. Significant torque and flux ripple reduction, rise time optimization, and the minimization of stator and rotor current signal harmonics are some of these enhancements. We can make the following deductions based on the results:

1. The suggested control method provides good static and dynamic system performance, according to simulation results.
2. The doubly supplied induction motor is guaranteed to decouple its electromagnetic flux and torque.
3. The SVM technique performs noticeably better than the conventional DTC technique by lowering torque and flux ripples, which lessens motor issues (heating, mechanical vibration, aging, etc.).

Declaration of Generative AI and AI-assisted Technologies in the Writing Process

The authors wrote, reviewed and edited the content as needed and verifies that none utilized artificial intelligence (AI) tools were used. The authors take full responsibility for the content of the publication.

References:

[1] I. Lopez-Garcia, G. Espinosa-Perez, H. Siguerdidjane, A. Doria-Cerezo, On the passivity-based power control of a doubly-fed induction machine, *International Journal Electrical Power and Energy Systems,* Vol. 45, pp.303-312, 2013.

[2] M. Taoussi, M. Karim, B. Bossoufi, D. Hammoumi, A. Lagrioui, Speed backstepping control of the double-fed induction machine drive, *Journal of theoretical and applied information technology,* Vol.74 No.2, pp.189-199, 2015.

[3] N. Bounar, A. Boulkroune, F. Boudjema, M. Farza, Adaptive fuzzy vector control for a doubly-fed induction motor, *Neurocomputing,* pp.756–769, 2015.

[4] F. Blaschke, The principle of field orientation as applied to the new transvector closed-loop control system for rotating machines, *Siemens Review,* Vol. 39, No. 5, pp. 217–220, 1972.

[5] A. Alwadie, A Concise Review of Control Techniques for Reliable and Efficient Control of Induction Motor, *International Journal of Power Electronics and Drive System (IJPEDS),* Vol. 9, No. 3, pp. 1124-1139, 2018.

[6] T. Sutikno, Idris NRN, A. Jidin, A review of direct torque control of induction motors for sustainable reliability and energy efficient drives, *Renewable Sustainable Energy Review,* Vol. 32, pp. 548–58, 2014.

[7] Takahashi, T. Noguchi, A new quick-response and high-efficiency control strategy of an induction motor, *IEEE Trans. on Ind. Appl.,* Vol.22, No.5, pp.820-827, 1986.

[8] M. Depenbrock, Direct Self Control (DSC) of Inverter Fed Induction Machine, *IEEE Trans. on Power Electronics,* Vol. 3, No.4, pp.420-429, 1988.

[9] F. Bonnet, P.E. Vidal, and M. Pietrzak-David, Direct torque control of doubly fed induction machine, *Bulletin of the polish academy of sciences technical sciences,* Vol. 54, No. 3, 2006.

[10] A. Ammar, A. Bourek, A. Benakcha, Sensorless SVM-direct torque control for induction motor drive using sliding mode observers, *J Control Autom Electr Syst,* 2016.

[11] F. Boumaraf, M.L. Bendaas, R. Abdessemed, and S. Belkacem, Direct Torque Control of Doubly Fed Induction Machine, *International Journal on Electrical Engineering and Informatics,* Vol.7, No.3, pp. 541-555, 2015.

[12] M. H. Lazreg and A. Bentaallah, Sensorless Speed Control of Double Star Induction Machine with Five Level DTC Exploiting Neural Network and Extended Kalman Filter, *Iranian Journal of Electrical and Electronic Engineering,* Vol. 15, No. 1, pp. 142–150, 2019.

[13] Q. M. Attique, Y. Li, and K. Wang, A Survey on Space-Vector Pulse Width Modulation for Multilevel Inverters, *CPSS Transactions on Power Electronics and Applications,* Vol. 2, No. 3, pp. 226–236, September 2017.

[14] H. Yu1, Z. Chen, Three-Phase Induction Motor DTC-SVPWM Scheme with Self-tuning PI-Type Fuzzy Controller, *International Journal of Computer and Communication Engineering,* Vol. 4, No. 3, pp. 204–210, May 2015.

[15] Dj. Cherifi and Y. Miloud, Speed Sensorless Control of a Doubly Fed Induction Motor Drives using MRAS Estimator, *International Journal of Electrical Components and Energy Conversion,* Vol.4, No.1, pp. 1–12, 2018.

[16] M. T. Lazim, M. J. M. Al-khishali and A. I. Al-Shawi, Space Vector Modulation Direct Torque Speed Control Of Induction Motor, *The 2nd International Conference on Ambient Systems, Networks and Technologies, Procedia Computer Science,* pp.505–512, 2011.

[17] Y. Zahraoui, M. Akherraz, C. Fahassa, Induction motor DTC performance improvement by reducing torque ripples in low speed, *U.P.B. Sci. Bull., Series C*, Vol. 81, Iss. 3, 2019.

[18] N. El Ouanjli , A. Derouich, A. EL Ghzizal, S. Motahhir, A. Chebabhi, Y. EL Mourabit and M. Taoussi, "Modern improvement techniques of direct torque control for induction motor drives - a review", *Protection and Control of Modern Power Systems,* 4:11, 2019,

[19] A. Zemmit, S. Messalti, A. Harrag, "A new improved DTC of doubly fed induction machine using GA-based PI controller", *Ain Shams Engineering Journal,* 2017.

[20] M. Said, A. Derouich, N. El Ouanjli, Mahmoud A. Mossa, M. Sagar Bhaskar, Ngo Kim Lan, Nguyen Vu Quynh, "A New Robust Direct Torque Control Based on a Genetic Algorithm for a Doubly-Fed Induction Motor: Experimental Validation", *Energies,* 15, 5384, 2022,

[21] H. F. Rashag, Nadia M.L. TAN, S.P. KOH, Ahmed N. Abdalla, K.H. Chong, S.K. Tiong, "DTC-SVM Based on PI Torque and PI Flux Controllers to Achieve High Performance of Induction Motor", *Research Journal of Applied Sciences, Engineering and Technology,* Vol. 7, No. 4, pp. 875-891, 2014

[22] M. Zaid Aihsan, A. Jidin, M. M. Azizan, M. Izuan Fahmi, K. Hasikin, "Flexible Sector Detector-Based Mismatch Supply Voltage in Direct Torque Control Doubly Fed Induction Machine: An Experimental Validation", *Alexandria Engineering Journal,* 74, 689–704, 2023.

[23] A. Ammar, A. Bourek, A. Benakcha, "Robust load angle direct torque control with SVM for sensorless induction motor using sliding mode controller and observer", *Int. J. Computer Aided Engineering and Technology,* Vol. 11, No. 1, pp.14-34, 2019,

[24] H. F. Rashag, S. P. Koh, K. H. Chong, S. K. Tiong, N. M. L. Tan and A. N. Abdalla, High performance of space vector modulation direct torque control SVM-DTC based on amplitude voltage and stator flux angle, *Research Journal of Applied Sciences, Engineering and Technology,* Vol. 5, No. 15, pp.3934-3940, 2013.

[25] L. Kyo-Beum, F. Blaabjerg, An improved DTC-SVM method for sensorless matrix converter drives using an over modulation strategy and a simple nonlinearity compensation, *IEEE Transactions on Industrial Electronics,* Vol. 54, No. 6, pp.3155-3166, 2007.

[26] A. K. Bilhan and E. Akbal, Modeling and simulation of two-level space vector PWM inverter using photovoltaic cells as DC source, *International Journal of Electronics, Mechanical and Mechatronics Engineering,* Vol. 2, No. 4, pp. 311–317, 2016.

[27] H. Benbouhenni, Z. Boudjema and A. Belaidi, Direct Vector Control of a DFIG Supplied by an Intelligent SVM Inverter for Wind Turbine System, *Iranian Journal of Electrical and Electronic Engineering,* Vol. 15, No. 1, pp. 45–55, 2019.

[28] Dj. Cherifi and Y. Miloud, Contribution to the Improvement of Sensorless DTC-SVM forThree-Level NPC Inverter-fed Induction Motor Drive, *WSEAS Transactions on Power Systems,* Vol.18, pp. 436–445, 2023.

APPENDIX

The parameter values of the DFIM used in this work are presented in Table 3:

Table 3. DFIM motor parameters

Variable	Symbol	Value (unit)
DFIM Mechanical Power	P_W	1.5 Kw
Nominal speed	ω	1450 rpm
Pole pairs number	P	2
Stator resistance	R_s	1.68 Ω
Rotor resistance	R_r	1.75 Ω
Stator self inductance	L_s	295 mH
Rotor self inductance	L_r	104 mH
Mutual inductance	L_m	165 mH
Moment of inertia	J	0.01 $kg.m^2$
friction coefficient	F	0.0027 $kg.m^2/s$
Nominal Frequency	f	50 Hz

Source: created by the authors

Contribution of Individual Authors to the Creation of a Scientific Article (Ghostwriting Policy)

The authors equally contributed in the present research, at all stages from the formulation of the problem to the final findings and solution.

Sources of Funding for Research Presented in a Scientific Article or Scientific Article Itself

No funding was received for conducting this study.

Conflict of Interest

The authors have no conflicts of interest to declare that are relevant to the content of this article.